DO THE MERCAPTOCARBENE (H–C–S–H) AND SELENOCARBENE (H–C–Se–H) CONGENERS OF HYDROXYCARBENE (H–C–O–H) UNDERGO 1,2-H-TUNNELING?

János SARKA[a1], Attila G. CSÁSZÁR[a2]* and Peter R. SCHREINER[b,]*

[a] *Laboratory of Molecular Spectroscopy and Department of Physical Chemistry, Institute of Chemistry, Loránd Eötvös University, H-1518 Budapest 112, P.O. Box 32, Hungary; e-mail: [1] sarkajanos@gmail.com, [2] csaszar@chem.elte.hu*

[b] *Institute für Organische Chemie der Justus-Liebig-Universität, Heinrich-Buff-Ring 58, D-35292 Giessen, Germany; e-mail: prs@org.chemie.uni-giessen.de*

Received March 1, 2011
Accepted April 13, 2011
Published online May 3, 2011

Dedicated to our colleague Zdeněk Havlas for his contributions to computational chemistry and on the occasion of his 60th birthday.

The principal purpose of this investigation is the determination of the tunneling half-lives of the *trans*-HCSH → H_2CS and the *trans*-HCSeH → H_2CSe unimolecular isomerization reactions at temperatures close to 0 K. To aid these determinations, accurate electronic structure computations were performed, with electron correlation treatments as extensive as CCSDT(Q) and basis sets as large as aug-cc-pCV5Z, for the isomers of [H,H,C,S] and [H,H,C,Se] on their lowest singlet surfaces and for the appropriate transition states yielding structural data for key stationary points characterizing the isomerization reactions. The computational results were subjected to a focal-point analysis (FPA) that yields accurate relative energies with uncertainty estimates. The tunneling half-lives were determined by a simple Eckart-barrier approach and via the more sophisticated though still one-dimensional Wentzel–Kramers–Brillouin (WKB) approximation. Only stationary-point information is needed for the former while an intrinsic reaction path (IRP) is necessary for the latter approach. Both protocols suggest that, unlike for the parent hydroxymethylene (HCOH), at the low temperatures of matrix isolation experiments no tunneling will be observable for the *trans*-HCSH and *trans*-HCSeH systems.

Keywords: Carbenes; Mercaptocarbene (HCSH); Selenocarbene (HCSeH); Tunneling; Eckart barrier; WKB approximation; *ab initio* calculations; Hydrogen transfer.

Apart from being the parent and the first hydroxycarbene ever synthesized[1], a special property of *trans*-H–C–OH (in its $\tilde{X}^1A'$ electronic state) is that it very efficiently undergoes quantum mechanical hydrogen tunneling

doi:10.1135/cccc2011053

(1,2-H-shift) to formaldehyde (H_2CO), even at very low temperatures. This efficient unimolecular isomerization reaction, with an experimental tunneling half-life of about 2 h in noble gas matrices at temperatures as low as 11 K, takes place under a barrier of record size, around 30 kcal mol^{-1} [1,2]. In anticipation of a possibly similar preparation and follow-up detection of the H–C–SH and H–C–SeH congeners of hydroxymethylene, a concerted theoretical effort is made here to characterize the [H,H,C,S] and [H,H,C,Se] isomers (Fig. 1) relevant for the tunneling of *trans*-HCSH to H_2CS (thioformaldehyde) and *trans*-HCSeH to H_2CSe (selenoformaldehyde) and the tunneling rate itself.

Singlet thioformaldehyde ($\tilde{X}^1A_1$) is the global minimum on the ground electronic state potential energy hypersurface (PES) of the [H,H,C,S] species. Spectroscopic[3,4] and quantum chemical[5,6] studies suggest that at equilibrium the singlet-triplet energy separation of this isomer is large, about 40 kcal mol^{-1}. *Ab initio* electronic structure computations indicate for *trans*- and *cis*-mercaptocarbene, *t*-HCSH and *c*-HCSH, that the singlet states also lie by some 17 kcal mol^{-1} lower in energy than the corresponding triplet states. Therefore, we limit our present study to the singlet ground electronic state PES of [H,H,C,S]. Ochsenfeld et al.[6] observed symmetry-breaking problems for the singlet [H,H,C,S] isomers at the Hartree–Fock (HF)[7] and Møller–Plesset (MP2)[8] levels of theory (using a triple-zeta plus polarization basis), which is remedied at the coupled cluster (CC)[9,10] level. Tachibana et al.[11] reported, at the HF/6-31G** level, a non-planar transition state (TS) for the isomerization reaction of mercaptocarbene; non-planarity of the TS arises most likely due to a similar symmetry-breaking problem. These observations suggest the necessity of using high-level electronic structure treatments for computations of the stationary points on this PES in order to arrive at definitive results.

The spectrum of thioformaldehyde has been the subject of several experimental studies in the microwave (MW)[12–15], millimeter-wave[16], and infrared ranges[15,17–20]. The structure of H_2CS is very similar to that of formaldehyde (with a significantly shorter *r*(C–H) and an *r*(C=S) estimate of

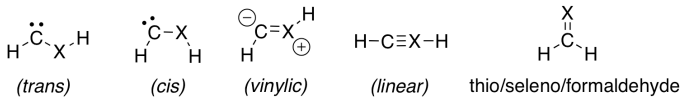

FIG. 1
Possible bonding situations in hydroxycarbene (X = O), mercaptocarbene (X = S), and selenocarbene (X = Se) as well as in formaldehyde and its congeners

1.611 Å [21]); it is an *a*-type asymmetric top molecule with a sizable dipole moment of 1.6491(4) D [22]. A quartic internal coordinate force field of H_2CS has been determined by Martin et al.[23] at the frozen-core CCSD(T)/cc-pVTZ level. This force field was reexpanded and refined by Carter and Handy[24] via variational nuclear motion computations, adjusting both the equilibrium structure and the force constants to 50 observed spectroscopic data. A dipole moment surface (DMS) was also developed for thioformaldehyde[25].

The structure and properties of mercaptocarbene are much less well studied. This is true despite the fact that this molecule is of considerable astrophysical interest as one of the simplest organosulfur molecules. Moreover, the recent matrix isolation and spectroscopic as well as computational characterization of H–CS–OH brought interesting bonding aspects of such formal CS adducts (H_2CS = CS + H_2; H–CS–OH = CS + H_2O) to the fore[26,27]. By comparison of bond lengths, vibrational frequencies, and compliance force constants, H–CS–OH possesses a strong double or a weak triple bond. Although one of the resonance structures can be best viewed as a carbene (H–C̈–S–OH), this resonance contributor practically does not play a role. It is therefore open to discussion what kind of bonding dominates mercaptocarbene (X = S in Fig. 1): carbene-type (*trans* and *cis*), vinylidene-like, or linear with a triple bond, and what factors determine the actual bonding type. This bonding analysis of mercaptocarbene, augmented with a fresh look at some of the structural and energetic characteristics of the singlet isomers of [H,H,C,S], forms part of the present study.

Selenoformaldehyde ($\tilde{X}^1A_1$) is the global minimum on the ground electronic state PES of the [H,H,C,Se] species. Despite several experimental[28–32] and first-principles[32–37] studies, characterization of this PES received less attention than that of [H,H,C,S]. Following the first successful preparation of selenoformaldehyde in the gas phase[38], Collins et al.[33] reported HF and limited electron correlation results on the electronic structure of H_2C=Se. They found that the order of orbital occupancies in H_2C=Se is entirely analogous to that found in H_2C=O and H_2C=S. Furthermore, they showed that the singlet-triplet energy separation characterizing this [H,H,C,Se] isomer is large, on the order of 33 kcal mol^{-1}. Therefore, similarly to [H,H,C,S], we limit our present study to the singlet ground electronic state PES of [H,H,C,Se]. In a more recent study, Leszczynski et al.[37] carried out post-HF electronic structure computations and determined improved molecular parameters (including structures and harmonic vibrational wavenumbers) for the set {H_2CO, H_2CS, H_2CSe}. Measurement of the MW spectrum of selenoformaldehyde by Brown et al.[28] resulted in an effective structure of

H_2C=Se, with an *r*(C=Se) estimate of 1.759 Å and an unphysical HCH bond angle of 120.4° (compare to 116.6° and 116.3° for CH_2=O[21] and CH_2=S[12], respectively) and a dipole moment further decreasing from that of formaldehyde, 2.33 D[22], to 1.41(1) D. Beckers et al.[32] measured the infrared spectrum of matrix-isolated selenoformaldehyde resulting in all six fundamentals and two combination bands. The photoelectron spectrum of H_2CSe was also recorded[29].

Missing almost completely from previous theoretical studies, except ref.[11], is the investigation of the isomerization of *t*-HCXH to H_2CX (X = S or Se), either thermally or through H-tunneling. There is a transition-state investigation for the X = S system due to Yamada et al.[39], but it is concerned with the *cis–trans* HCSH interconversion and not the isomerization reaction. Not even introductory studies exist for *cis–trans* HCSeH and its isomerization reaction. Tunneling via a 1,2-H-shift mechanism is the main subject of the present study and all other first-principles structural and energetic results were generated in order to make the present tunneling investigation definitive.

COMPUTATIONAL DETAILS

The atom-centered Gaussian basis sets selected for the electronic structure computations of this study contain polarization, diffuse, and core functions, all needed for the determination of accurate molecular structures, energies, and properties[40]. The correlation-consistent, polarized, core-valence aug-cc-pCV*n*Z and aug-cc-pwCV*n*Z, *n* = 2(D), 3(T), 4(Q), 5, basis sets of Dunning and co-workers[41–44] were employed throughout this study. The augmented (aug) basis sets contain diffuse functions, while tight functions necessary for treating core correlation are contained in the core-polarized (C) part of the bases. These atomic-orbital basis sets provide superior performance in approaching the complete basis set (CBS) limit in a systematic fashion during traditional electronic structure computations. For the [H,H,C,S] isomers the aug-cc-pCVDZ, aug-cc-pCVTZ, aug-cc-pCVQZ and aug-cc-pCV5Z basis sets contain 81, 180, 335 and 558 contracted Gaussian functions (CGFs), respectively. For the [H,H,C,Se] isomers the {aug-cc-pwCVDZ, aug-cc-pwCVTZ, aug-cc-pwCVQZ, aug-cc-pwCV5Z} basis sets employed contain {97, 205, 371, 604} CGFs. Only pure spherical harmonics were employed in all basis sets. Note that smaller versions of the correlation-consistent basis sets, e.g., cc-pVDZ, cc-pVTZ, and cc-pV(T+d)Z (for S), were also employed.

Electronic wave functions were determined in this study by the single-configuration, self-consistent-field, restricted Hartree–Fock (RHF) method[7] and by coupled cluster (CC) methods[9,10,45], including all single and double (CCSD)[46] and all single, double, and triple (CCSDT)[47] excitations, as well as a perturbative correction for connected triple [CCSD(T)][48] and quadruple [CCSDT(Q)][49,50] excitations.

To determine accurate relative energies of the optimized stationary points, the focal-point analysis (FPA) approach[51–53] was utilized. The FPA approach has been employed, among many other systems, for a number of carbenes[54–56]. Extrapolation of the energies to the CBS limit at the RHF, CCSD and CCSD(T) levels were performed, as part of the FPA approach. For RHF, the total energy was extrapolated using the three-parameter exponential formula $E_n = E_{CBS} + A \exp(-Bn)$ with $n \in \{3,4,5\}$, where A and B are adjustable parameters, E_n is the RHF total energy for a correlation-consistent basis set aug-cc-pCVnZ, and E_{CBS} is the Hartree–Fock limit. For CCSD and CCSD(T), the correlation energies (ε_n) were extrapolated according to the two-parameter inverse-cubic, polynomial formula $\varepsilon_n = \varepsilon_{CBS} + Cn^{-3}$, where C is an adjustable parameter. Higher-order energy corrections were treated additively, assuming that these corrections do not change significantly with the size of the basis. As to the auxiliary corrections normally included within the FPA approach, the core correlation term is not included here as all electrons (except the 1s electrons of S and the 1s, 2s, and 2p electrons of Se) were treated *a priori*. The MVD1 relativistic corrections[57,58] were obtained at the CCSD(T)/aug-cc-pCVTZ and CCSD(T)/aug-cc-pwCVTZ levels for [H,H,C,S] and [H,H,C,Se], respectively, while the diagonal Born–Oppenheimer corrections (DBOC) were deemed to be negligible and thus were not computed.

The structures and the quadratic force fields of the [H,H,C,S] and [H,H,C,Se] isomers were determined using analytic geometric derivatives[59–61]. The structures and force fields for the [H,H,C,S] isomers and the transition state TS1 connecting the minima *t*-HCSH and H_2CS were determined at the all-electron (AE) CCSD(T)/aug-cc-pCVQZ level of electronic structure theory. The structures and the quadratic force fields of the [H,H,C,Se] isomers and the transition state TS2 connecting *t*-HCSeH to H_2CSe were determined at the CCSD(T)_AE/aug-cc-pwCVQZ level of electronic structure theory. The geometry optimizations, also yielding the fixed reference structures for the force field expansions and the focal-point analyses, and all computations up to CCSDT utilized the electronic structure code CFOUR [62]. The CCSDT(Q) computations were performed with the help of the MRCC code[45,63] interfaced to CFOUR.

Use of the Wentzel–Kramers–Brillouin (WKB) approximation[64,65] requires the availability of a potential function corresponding to an intrinsic reaction path (IRP) following the one-dimensional intrinsic reaction coordinate (IRC)[66]. Application of the WKB method for the purpose of computing tunneling half-lives consists of the following steps: (i) step-by-step computation of an IRP connecting the TS to the reactant and product, followed by a polynomial fit to the energy points corresponding to certain positive (on the product side) and negative (on the reactant side) values of the IRC, (ii) determination of the energy-dependent barrier penetration integrals and the related barrier transmission probabilities, (iii) establishment of the tunneling rate constant at a fixed energy, and (iv) calculation of the tunneling half-life assuming the validity of first-order kinetics. Generation of the IRPs followed the prescriptions of ref.[67] and employed the CFOUR code. Application of a reaction path Hamiltonian[68] along an IRP requires the computation of vibrational frequencies for modes orthogonal to the path. This task demands attention to numerous subtle issues detailed in ref.[69].

The time-independent Schrödinger equation can be solved analytically for the model Eckart potential[70] yielding a simple analytic form for the transmission probability and thus for the tunneling rate constant. Computation of the tunneling rates based on the Eckart-barrier and WKB approaches were performed with codes written in MATHEMATICA[71].

Note that both in the WKB and Eckart approaches the tunneling rate constant is the product of the transmission probability and the frequency of the reaction mode. Furthermore, temperature dependence of the tunneling half-life can be computed via Boltzmann averaging.

RESULTS AND DISCUSSION

Structure/Bonding

The equilibrium Born–Oppenheimer[73] r_e^{BO}(CH) bond length changes very little in the CH_2X (X = O, S, Se) series. The largest value, r_e^{BO}(CH) = 1.101 Å is in formaldehyde, decreasing to 1.086 Å in thioformaldehyde, and further to 1.083 Å in selenoformaldehyde. The equilibrium HCH bond angle is also as expected based on VSEPR arguments[74], 116.3(3)° in $H_2C{=}O$ [75], 117.2(4)° in $H_2C{=}S$ [18], and 117.1° in $H_2C{=}Se$ (the difference in the r_z-type bond angle[73] reported for H_2CS and the r_e-type bond angle should be on the order of 0.1°).

Overall, the structure of thioformaldehyde is very similar to that of formaldehyde, as it displays a normal CH bond length, a normal HCH bond

TABLE I

Equilibrium structural parameters (distances, r_e, in Å and angles, $\angle_e$, in °), equilibrium rotational constants (A_e, B_e, and C_e, in MHz), and dipole moments (μ, in D) of the H_2CS isomers and the transition state (TS1) of the *t*-HCSH → H_2CS unimolecular isomerization reaction, all obtained at the all-electron CCSD(T)/aug-cc-pCVQZ level of electronic structure theory. The relative energies (in kcal mol^{-1}) reported refer to final estimates from an FPA analysis (see Table II). PG, point-group symmetry of the stationary point

Structure (PG)	Structural data[a]	Rotational constants[b]	Dipole moments	Relative energy
H_2CS	r_e(CS) = 1.6101	A_e = 294637.8	μ_{tot} = 1.694	0.00
(C_{2v})	r_e(CH) = 1.0856	B_e = 17748.6		
	$\angle_e$(SCH) = 121.82	C_e = 16740.2		
t-HCSH	r_e(CS) = 1.6496	A_e = 188779.6	μ_{tot} = 1.838	43.93(20)
(C_s)	r_e(CH) = 1.1036	B_e = 19022.9	μ_a = 1.743	
	r_e(SH) = 1.3474	C_e = 17280.9	μ_b = 0.582	
	$\angle_e$(SCH) = 102.71		μ_c = 0.000	
	$\angle_e$(CSH) = 100.18			
c-HCSH	r_e(CS) = 1.6324	A_e = 194237.8	μ_{tot} = 2.641	44.93(21)
(C_s)	r_e(CH) = 1.0958	B_e = 19007.5	μ_a = 1.553	
	r_e(SH) = 1.3674	C_e = 17313.2	μ_b = 2.136	
	$\angle_e$(SCH) = 111.03		μ_c = 0.000	
	$\angle_e$(CSH) = 109.58			
TS1	r_e(CS) = 1.7028			77.09(36)
(C_s)	r_e(CH) = 1.0982			
	r_e(SH) = 1.4490			
	$\angle_e$(SCH) = 113.75			
	$\angle_e$(CSH) = 53.15			

[a] The CCSD(T)_AE/aug-cc-pwCVQZ structural results for H_2CS are basically the same as reported in the Table, the only difference is in r_e(CS), which is 1.6095 Å at this level. The "empirical" equilibrium geometry parameters of H_2CS reported in ref.[24] are r_e(CS) = 1.6110 Å, r_e(CH) = 1.0856 Å, and $\angle_e$(SCH) = 121.88°. [b] The experimental ground-state rotational constants of $H_2{}^{12}C^{32}S$, in MHz, are as follows: A_0 = 291 710(23), B_0 = 17 698.87(44), and C_0 = 16 652.98(48)[14]. Appending CCSD(T)_FC/cc-pVTZ first-order vibrational-rotational interaction constants, determined via formulas of second-order vibrational perturbation theory (VPT2), to the equilibrium rotational constants reported in the Table results in the following computational estimates of the ground-state rotational constants of $H_2{}^{12}C^{32}S$: A_0 = 292 703.5, B_0 = 17 671.3, and C_0 = 16 630.0 MHz.

angle, and a CS double bond with r_e^{BO}(CS) = 1.610 Å (Tables I and VII and Fig. 2), which is the prototypical equilibrium Born–Oppenheimer C=S double bond length. The CS bond length in HCSH, *cis* or *trans* (Tables I and VII), is characteristic of a slightly elongated double bond, with a bond length of about 1.64 Å (for *c*-HCSH the CS bond length is only 1.63 Å). Thus, based on this bond length information alone one could conclude that the most reasonable description of HCSH is a vinylic form (Fig. 1) owing to the electropositive nature and the high polarizability of S. This structural characteristics should be compared to that of the parent hydroxycarbene, HCOH. The CO bond length in *t*-HCOH computed at a similar level of theory, all-electron CCSD(T)/cc-pCVQZ, is 1.31 Å, while the typical equilibrium, r_e^{BO}, single and double CO bond lengths are 1.42 and 1.21 Å, respectively (Table VII). Thus, the bond in HCSH is weaker than a double bond but not as weak as that in HCOH. This suggests a clearly carbene-like C atom in HCOH but an ylidic structure for the much more polar *c*- and *t*-HCSH. This observation predicts that H-tunneling in HCSH might be much less efficient than that in HCOH.

Sulfur is known to be a particularly good candidate for multiple bonding[76]. Schreiner and co-workers[26] have recently investigated H–CS–OH and suggested that its CS bond should be considered as a weak triple or a stron-

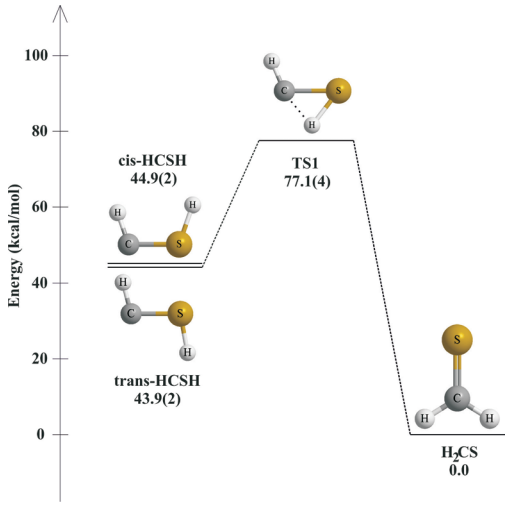

FIG. 2
One-dimensional representation of the relevant stationary points on the PES of the [H,H,C,S] system whose relative energies were investigated in this study via the FPA scheme

TABLE II

Focal-point analysis of the energy differences (in kcal mol^{-1}) between *t*-HCSH and H_2CS, between *c*-HCSH and *t*-HCSH, and between the transition state (TS1), leading from *t*-HCSH to H_2CS, and *t*-HCSH[a]

X = S	ΔE_e(HF)	δ[CCSD]	δ[CCSD(T)]	δ[CCSDT]	δ[CCSDT(Q)]	ΔE_e(FCI)
t-HCSH – H_2CS						
aug-cc-pCVDZ(81)	42.23	3.73	0.25	–0.31	0.08	
aug-cc-pCVTZ(180)	41.53	3.84	0.43	–0.32		
aug-cc-pCVQZ(335)	41.38	4.00	0.45			
aug-cc-pCV5Z(558)	41.39	4.04	0.46			
Extrapolation	exp	pol3	pol3	add	add	
CBS	41.39	4.08	0.47	–0.32	0.08	45.70
Relativistic						+0.03
ZPVE						–1.80
Final estimate						**43.93(20)**
c-HCSH – *t*-HCSH						
aug-cc-pCVDZ	2.43	–0.31	–0.08	0.00	–0.02	
aug-cc-pCVTZ	2.08	–0.32	–0.09	0.00		
aug-cc-pCVQZ	2.02	–0.39	–0.09			
aug-cc-pCV5Z	2.02	–0.40	–0.09			
Extrapolation	exp	pol3	pol3	add	add	
CBS	2.02	–0.42	–0.09	0.00	–0.02	1.49
Relativistic						–0.05
ZPVE						–0.44
Final estimate						**1.00(5)**
TS1 – *t*-HCSH						
aug-cc-pCVDZ	47.97	–11.17	–2.59	0.07	–0.39	
aug-cc-pCVTZ	49.46	–11.59	–3.02	0.18		
aug-cc-pCVQZ	49.70	–11.63	–3.11			
aug-cc-pCV5Z	49.72	–11.59	–3.13			
Extrapolation	exp	pol3	pol3	add	add	
CBS	49.72	–11.56	–3.16	0.18	–0.39	34.79
Relativistic						–0.12
ZPVE						–1.51
Final estimate						**33.16(30)**

[a] The reference structures are fixed during the focal-point analysis and were obtained at the CCSD(T)/aug-cc-pCVQZ level (see Table I for the actual structural values). The harmonic zero-point vibrational energies, obtained at the CCSD(T)/aug-cc-pCVQZ level, are 15.52, 13.72 and 13.28 kcal mol^{-1} for the global minimum, the *trans* and the *cis* forms, respectively. CBS, complete basis set limit. The zero-point vibrational energy (ZPVE) of TS1, excluding the imaginary mode, is 10.85 kcal mol^{-1}, while excluding the related mode for *t*-HCSH results in a ZPVE estimate of 12.36 kcal mol^{-1}. exp, extrapolation according to the three-parameter exponential formula (see text); pol3, extrapolation according to a two-parameter inverse-cubic polynomial formula (see text); add, additivity assumption based on the largest basis result.

ger than typical double bond. One can investigate the structure of the parent compound, H–C≡O–OH, and determine the bond lengths there. B3LYP/6-311+G(d,p) optimizations[77,78], performed as part of this study, reveal that the CO bond length in H–CO–OH, about 1.16 Å both in the *trans* and the *cis* forms, is much stronger than a double bond (r_e^{BO} = 1.206 Å in H_2CO) but weaker than a triple bond (r_e^{BO} = 1.13 Å in CO). In fact, based just on the CO bond length, the bond order is about 2.5, similar to what was determined for the bond order of H–C≡S–OH. These findings can be rationalized through the OH group withdrawing electrons from the formal carbene-like C atom to the CO bond in H–C≡O–OH making it considerably stronger. This also means that just as H–CS–OH, H–CO–OH should not be considered as a carbene.

The typical equilibrium length of the C=Se double bond is that computed for H_2CSe, r_e^{BO} = 1.75 Å (Table IV and Fig. 3). The CSe bond length in HCSeH, *cis* or *trans* (Tables IV and VII), is characteristic of a slightly elongated double bond, with a bond length of about 1.80 Å (for *c*-HCSeH the CSe bond length is only 1.78 Å). Thus, the bonding situation in the relevant [H,H,C,S] and [H,H,C,Se] isomers is quite similar. Again, it seems that HCSeH should not be viewed as a typical carbene. These arguments receive further support when one compares the single, double, and triple bond

TABLE III

Harmonic vibrational wavenumbers, ω_i in cm^{-1} and band intensities, in km mol^{-1}, given in parentheses, computed at the all-electron CCSD(T)/aug-cc-pCVQZ level for the singlet isomers of the [H,H,C,S] system investigated in this study and for the transition state (TS1) connecting the minima *t*-HCSH and H_2CS

No.	H_2CS[a]		*t*-HCSH		*c*-HCSH		TS1	
ω_1	A_1	3089.4(24.4)	*A′*	2992.0(22.4)	*A′*	3058.1(14.9)	*A′*	2989.4
ω_2	A_1	1496.4(2.3)	*A′*	2604.1(6.9)	*A′*	2433.2(86.0)	*A′*	2199.0
ω_3	A_1	1077.8(8.0)	*A′*	1177.3(11.4)	*A′*	1107.7(3.8)	*A′*	1083.1
ω_4	B_1	1006.2(39.8)	*A′*	954.4(7.8)	*A′*	965.6(19.9)	*A′*	841.4
ω_5	B_2	3181.2(24.4)	*A′*	885.1(29.8)	*A′*	790.1(33.8)	*A′*	1869.0*i*
ω_6	B_2	1004.0(1.8)	*A″*	984.3(20.3)	*A″*	935.8(6.2)	*A″*	477.8

[a] The measured gas-phase band positions[18] (in cm^{-1}) are as follows: ν_1 = 2971.0, ν_2 = 1457.3, ν_3 = 1059.2, ν_4 = 990.2, ν_5 = 3024.6, and ν_6 = 991.0. Appending CCSD(T)_FC/cc-pVTZ anharmonic vibrational corrections, determined via formulas of second-order vibrational perturbation theory (VPT2), to the computed harmonic frequencies reported in the Table results in the following computational estimates of the anharmonic vibrational fundamentals: ν_1 = 2975.4, ν_2 = 1454.2, ν_3 = 1062.4, ν_4 = 992.0, ν_5 = 3027.7, and ν_6 = 990.9 cm^{-1}.

TABLE IV

Equilibrium structural parameters (distances, r_e, in Å and angles, $\angle_e$, in °), equilibrium rotational constants (A_e, B_e, and C_e, in MHz), and dipole moments (μ, in D), of the H_2CSe isomers and the transition state (TS2) of the *t*-HCSeH → H_2CSe unimolecular isomerization reaction, all obtained at the all-electron CCSD(T)/aug-cc-pwCVQZ level of electronic structure theory. The relative energies (in kcal mol^{-1}) reported refer to final estimates from an FPA analysis. PG, point-group symmetry of the stationary point

Structure (PG)	Structural data	Rotational constants[a]	Dipole moments	Relative energy
H_2CSe	r_e(CSe) = 1.7519	A_e = 293754.6	μ_{tot} = 1.509	0.00
(C_{2v})	r_e(CH) = 1.0831	B_e = 12439.9		
	$\angle_e$(SeCH) = 121.46	C_e = 11934.5		
t-HCSeH	r_e(CSe) = 1.8000	A_e = 161229.2	μ_{tot} = 1.976	47.60(30)
(C_s)	r_e(CH) = 1.1065	B_e = 13521.8	μ_a = 1.851	
	r_e(SeH) = 1.4732	C_e = 12475.5	μ_b = 0.691	
	$\angle_e$(SeCH) = 101.39		μ_c = 0.000	
	$\angle_e$(CSeH) = 97.73			
c-HCSeH	r_e(CSe) = 1.7842	A_e = 166080.3	μ_{tot} = 2.525	48.19(32)
(C_s)	r_e(CH) = 1.0992	B_e = 13540.9	μ_a = 1.693	
	r_e(SeH) = 1.4931	C_e = 12520.1	μ_b = 1.874	
	$\angle_e$(SeCH) = 108.22		μ_c = 0.000	
	$\angle_e$(CSeH) = 107.76			
TS2	r_e(CSe) = 1.8648			77.34(50)
(C_s)	r_e(CH) = 1.0990			
	r_e(SeH) = 1.5554			
	$\angle_e$(SeCH) = 110.78			
	$\angle_e$(CSeH) = 50.75			

[a] The experimental ground-state rotational constants of $H_2{}^{12}C^{80}Se$, in MHz, are as follows: A_0 = 294 803(1870), B_0 = 12 404.01(4), and C_0 = 11 878.393(4)[28]. Appending frozen-core CCSD(T)/cc-pVTZ first-order vibrational-rotational interaction constants, determined via formulas of second-order vibrational perturbation theory (VPT2), to the equilibrium rotational constants reported in the Table results in the following computational estimates of the ground-state rotational constants of $H_2{}^{12}C^{80}Se$: A_0 = 292 017.3, B_0 = 12 383.5, and C_0 = 11 860.6 MHz.

lengths, computed and measured, in the C–X (X = O, S, Se) series[20,27,72,79–83] as presented in Table VII.

Energetics

There is nothing surprising in the FPA numbers of Tables II and V except the large δ[CCSDT] corrections in the case of the energy differences between the global minima, H_2CX, and *t*-HCXH, X = S and Se. The reason for this behavior is unclear but since the computations were extended to CCSDT(Q) this has no substantial effect on the accuracy of the FPA relative energies determined in this study though it increases the uncertainty of these particular computed relative energies.

The effective barriers for the *t*-HCSH → H_2CS and the *t*-HCSeH → H_2CSe reactions are almost the same as for the *t*-HCOH/H_2CO isomerization. With a conservative uncertainty estimate, the barrier heights on the reactant side are 33.15 ± 0.30 and 29.74 ± 0.40 kcal mol^{-1} for the S and Se congeners, respectively.

The computed energy difference between the global minimum, H_2CS, and *t*-HCSH, is 43.93 ± 0.20 kcal mol^{-1} (Table II and Fig. 2). This value is somewhat smaller than the analogous energy difference of 52 kcal mol^{-1} re-

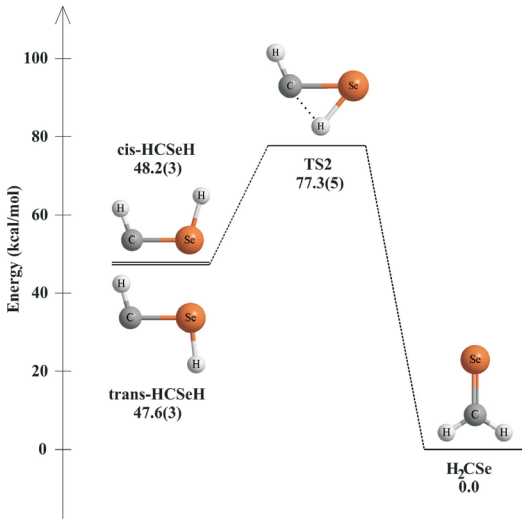

FIG. 3
One-dimensional representation of the relevant stationary points on the PES of the [H,H,C,Se] system whose relative energies were investigated in this study via the FPA scheme

TABLE V

Focal-point analysis of the energy differences (in kcal mol^{-1}) between *t*-HCSeH and H_2CSe, between *c*-HCSeH and *t*-HCSeH, and between the transition state (TS2), leading from *t*-HCSeH to H_2CSe, and *t*-HCSeH[a]

X = Se	ΔE_e(HF)	δ[CCSD]	δ[CCSD(T)]	δ[CCSDT]	δ[CCSDT(Q)]	ΔE_e(FCI)
t-HCSeH – H_2CSe						
aug-cc-pwCVDZ(97)	43.75	3.81	0.31	–0.40	0.09	
aug-cc-pwCVTZ(205)	44.84	3.96	0.49			
aug-cc-pwCVQZ(371)	44.87	4.32	0.53			
aug-cc-pwCV5Z(604)	44.89	4.40	0.54			
Extrapolation	exp	pol3	pol3	add	add	
CBS	44.89	4.49	0.55	–0.40	0.09	49.62
Relativistic						+0.32
ZPVE						–2.34
Final estimate						**47.60(30)**
c-HCSeH – *t*-HCSeH						
aug-cc-pwCVDZ	1.57	–0.13	–0.08	0.00	–0.01	
aug-cc-pwCVTZ	1.45	–0.12	–0.08			
aug-cc-pwCVQZ	1.43	–0.15	–0.08			
aug-cc-pwCV5Z	1.43	–0.16	–0.08			
Extrapolation	exp	pol3	pol3	add	add	
CBS	1.43	–0.17	–0.08	0.00	–0.01	1.17
Relativistic						–0.19
ZPVE						–0.39
Final estimate						**0.59(10)**
TS2 – *t*-HCSeH						
aug-cc-pwCVDZ	47.04	–11.19	–2.86	0.11	–0.47	
aug-cc-pwCVTZ	46.96	–11.41	–3.19			
aug-cc-pwCVQZ	47.01	–11.51	–3.28			
aug-cc-pwCV5Z	47.02	–11.52	–3.30			
Extrapolation	exp	pol3	pol3	add	add	
CBS	47.02	–11.54	–3.33	0.11	–0.47	31.79
Relativistic						–0.64
ZPVE						–1.41
Final estimate						**29.74(40)**

[a] The fixed reference structures for the focal-point analysis were obtained at the all-electron CCSD(T)/aug-cc-pwCVQZ level (see Table IV for the actual structural values). The harmonic zero-point vibrational energies, obtained at the CCSD(T)/aug-cc-pwCVQZ level, are 15.07, 12.73 and 12.34 kcal mol^{-1} for the global minimum, the *trans* and the *cis* forms, respectively. CBS, complete basis set limit. The zero-point vibrational energy (ZPVE) of the TS2, excluding the imaginary mode, is 10.11 kcal mol^{-1}, while excluding the related mode for *t*-HCSeH results in a ZPVE estimate of 11.52 kcal mol^{-1}. exp, extrapolation according to a three-parameter exponential formula (see text); pol3, extrapolation according to a two-parameter inverse-cubic formula (see text); add, additivity assumption based on the largest basis result.

ported for the *t*-HCOH/H_2CO pair[1]. The *t*-HCSeH – H_2CSe energy difference is 47.60 ± 0.30 kcal mol^{-1} (Table V and Fig. 3), in between the previously mentioned two values.

The FPA energy difference between the *cis* and the *trans* forms of HCSH is very small, only 1.00 ± 0.05 kcal mol^{-1} (note that the ZPVE correction to this number is almost 0.5 kcal mol^{-1}). This energy difference is considerably smaller than that observed for HCOH, for which it is about 4.4 kcal mol^{-1}. This energy difference is even smaller for the X = Se congener, only 0.59 ± 0.10 kcal mol^{-1} between the *cis* and the *trans* forms of HCSeH. The much larger energy difference also reflects the bonding dissimilarity of *t*-HCOH and *t*-HCSH and *t*-HCSeH.

Overall, there is a considerable similarity between the profiles of the singlet ground electronic state potential energy surfaces of [H,H,C,O], [H,H,C,S], and [H,H,C,Se] and between the relative energies of the stationary points on these PESs. This can clearly be seen in Fig. 4 showing the computed intrinsic reaction paths (IRPs) for the three 1,2-H-shift reactions investigated. It is also clear from this figure that the shape of the transition state region is very similar for [H,H,C,S] and [H,H,C,Se] and that the barrier is considerably narrower for the parent [H,H,C,O] system. Thus, the tunneling half-lives for the X = S and X = Se unimolecular isomerization reactions

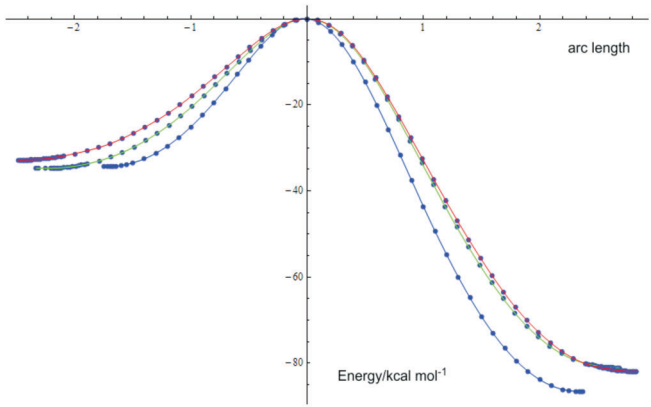

FIG. 4

One-dimensional computed intrinsic reaction paths for the [H,H,C,O] (blue), [H,H,C,S] (green), and [H,H,C,Se] (red) cases with common origin at the transition state and energy measured in kcal mol^{-1}. The negative and positive sides of the abscissa correspond to the reactant and product regions, respectively. See the Appendix for the functional forms of the curves

should be highly similar and much longer than that for the *t*-HCOH → H_2CO reaction.

Tunneling

The easiest way to determine the tunneling half-lives of the *t*-HCSH → H_2CS and *t*-HCSeH → H_2CSe unimolecular reactions goes via the Eckart-barrier approximation[70]. There are only a few quantities determining the tunneling lifetimes within this approach, all refering to the three stationary points characterizing the isomerization path.

In case of the tunneling from *t*-HCSH to H_2CS, the quantities determining the shape of the Eckart barrier are as follows: V_1 = 33.2 kcal mol^{-1}, V_2 = 77.1 kcal mol^{-1}, ω_{TS} = 1869*i* cm^{-1}, and ν_{vib} = 954.4 cm^{-1} (Tables II and III). Here V_1 and V_2 are the FPA barrier heights measured on the reactant and product sides, respectively, ω_{TS} is the imaginary frequency characterizing the transition state TS1, corresponding to the curvature at the top of the barrier, and ν_{vib} is the frequency of the vibrational normal mode of *t*-HCSH closest resembling the reaction mode. Note that it was not completely obvious, even for this seemingly simple case, which mode of the ω_3 – ω_4 dyad to select as the reaction mode but the normal-mode displacements suggest

TABLE VI
Harmonic vibrational wavenumbers, ω_i in cm^{-1}, and band intensities, in km mol^{-1}, given in parentheses, computed at the all-electron CCSD(T)/aug-cc-pwCVQZ level for the singlet isomers of the [H,H,C,Se] system investigated in this study and for the transition state (TS2) connecting the minima *trans*-HCSeH and H_2CSe

No.	H_2CSe[a]		*t*-HCSeH		*c*-HCSeH		TS2	
ω_1	A_1	3114.7(13.7)	A'	2965.7(29.6)	A'	3030.5(17.4)	A'	2989.1
ω_2	A_1	1462.8(2.1)	A'	2354.8(19.8)	A'	2218.0(93.0)	A'	2050.7
ω_3	A_1	878.1(1.3)	A'	1108.7(12.3)	A'	1036.4(4.1)	A'	1008.6
ω_4	B_1	939.2(48.5)	A'	847.2(6.6)	A'	810.7(29.2)	A'	657.4
ω_5	B_2	3219.3(0.2)	A'	728.1(20.1)	A'	676.4(11.3)	A'	1772.5*i*
ω_6	B_2	930.8(3.6)	A''	898.0(16.9)	A''	857.3(13.5)	A''	365.6

[a] The band positions measured in an Ar matrix (in cm^{-1}) are as follows: ν_1 = 2972.5, ν_2 = 1413.3, ν_3 = 854.2, ν_4 = 916.4, ν_5 = 3052.9, and ν_6 = 913.2. Appending CCSD(T)_FC/cc-pVTZ anharmonic vibrational corrections, determined via formulas of second-order vibrational perturbation theory (VPT2), to the computed harmonic frequencies reported in the Table results in the following computational estimates of the anharmonic vibrational fundamentals of H_2CSe: ν_1 = 2990.4, ν_2 = 1419.5, ν_3 = 865.7, ν_4 = 924.2, ν_5 = 3068.4, and ν_6 = 918.8 cm^{-1}.

the use of the ω_4 mode. Additional data for the Eckart-barrier calculation include the ZPVE estimates of the three stationary points (reactant, transition state, product) excluding the reaction mode. These correspond to the entries given in Table III. In the case of the tunneling from *t*-HCSeH to H_2CSe, the relevant quantities are as follows: V_1 = 29.7 kcal mol^{-1}, V_2 = 77.3 kcal mol^{-1}, ω_{TS} = 1772*i* cm^{-1}, and ν_{vib} = 847.2 cm^{-1} (Tables V and VII), where V_1 and V_2 are the FPA values.

Tunneling half-lives for the two systems and their deuterated isotopologues investigated were computed via the Eckart-barrier approximation at several levels of theory (Table VIII). The computed half-lives are most sensitive to the values of V_1 and ω_{TS}. Without any adjustment of the directly computed parameters given above, the tunneling half-life for *t*-HCSH is 2.4 × 10^6 h at 0 K, decreasing to 2.2 × 10^6 h at 11 K, a typical temperature of the matrix of common matrix-isolation experiments. The actual barrier height has a substantial effect on the tunneling half-life. Decreasing it to 32.9 kcal mol^{-1}, the lowest limit coming from the FPA analysis with a 2σ uncertainty estimate decreases the half-life to 1.5 × 10^6 h at 0 K. A further, unphysical decrease to 32.0 kcal mol^{-1} results in a half-life of 3.0 × 10^5 h at 0 K. By increasing the curvature at the top of the barrier, thus decreasing the width of the barrier, has an even more pronounced effect. Increasing ω_{TS} by a factor of 1.1 and 1.2, while keeping V_1 at 33.2 kcal mol^{-1}, decreases the tunneling half-lives to only 1.5 × 10^4 and 284 h at 0 K, respectively. The problem with these latter estimates is that such an increase in ω_{TS} should be considered completely unphysical due to the use of high levels of electronic structure theory in the present study. Thus, it can be concluded that at least within the one-dimensional Eckart-barrier approximation we cannot expect

TABLE VII

Computed (CCSD(T)/aug-cc-pCVQZ for X = O and S and CCSD(T)/aug-cc-pwCVQZ for X = Se) and experimental (in parentheses) CX (X = O, S, Se) bond lengths (in Å)

Bond type (species)	C–O	C–S	C–Se
Single (H_3C–XH)	1.418 (1.421[a])	1.811 (1.819[b])	1.950 (1.97[c])
Double (H_2C=X)	1.205 (1.206[d])	1.610 (1.611[e])	1.752 (1.759[f])
Triple (CX)	1.129 (1.128[g])	1.537 (1.535[h])	1.680 (1.676[i])
(*t*-HCXH)	1.311	1.650	1.800

[a] r_s from ref.[82], the estimate given in ref.[79] is 1.43 Å; [b] r_0 estimate from ref.[72]; [c] Ref.[79]; [d] Ref.[75]; [e] Ref.[21]; [f] Ref.[28], the estimate given in ref.[79] is 1.71 Å; [g] Ref.[83]; [h] Ref.[80]; [i] Ref.[80]

TABLE VIII
Comparison of the tunneling half-lives at 0 K (in h) of the different systems investigated via the WKB and Eckart-barrier approaches and employing structural and energetic results obtained at different levels of electronic structure theory

	HCOH[d]	HCSH	HCSD	HCSeH	HCSeD
WKB					
a) without ZPVE					
Ref. 1	13.6				
CCSD(T)_FC/cc-pVDZ		5.2×10^5		7.7×10^6	
CCSD(T)_FC/cc-pVTZ[a]		2.1×10^5		3.7×10^5	
b) with ZPVE					
Ref. 1	2.1				
CCSD(T)_FC/cc-pVDZ		7.6×10^4		1.7×10^6	
CCSD(T)_FC/cc-pVTZ[a]		2.7×10^4		5.0×10^4	
Eckart-barrier					
a) no scaling					
Ref. 1	114.4				
CCSD(T)_FC/cc-pVDZ		2.2×10^6	2.8×10^{15}	7.6×10^6	2.3×10^{16}
CCSD(T)_FC/cc-pVTZ[a]		4.3×10^6	6.9×10^{15}	3.6×10^6	8.2×10^{15}
CCSD(T)_AE/aug-cc-pCVQZ		4.3×10^6	7.2×10^{15}		
CCSD(T)_AE/aug-cc-pwCVQZ				1.2×10^6	1.8×10^{15}
FPA[b]		2.4×10^6	9.5×10^{14}	1.6×10^5	3.9×10^{13}
b) scaled[c]					
Ref. 1	2.1				
CCSD(T)_FC/cc-pVDZ		1.7×10^4	3.5×10^{12}	5.4×10^4	2.4×10^{13}
CCSD(T)_FC/cc-pVTZ[a]		3.2×10^4	7.8×10^{12}	2.7×10^4	9.3×10^{12}
CCSD(T)_AE/aug-cc-pCVQZ		3.2×10^4	8.1×10^{12}		
CCSD(T)_AE/aug-cc-pwCVQZ				1.0×10^4	2.4×10^{12}
FPA[b]		1.9×10^4	4.3×10^{12}	1.6×10^3	7.1×10^{10}

[a] In the HCSH and HCSD systems the cc-pV(T+d)Z basis set was employed. [b] The harmonic wavenumbers were computed at the all-electron CCSD(T) level with the aug-cc-pCVQZ and aug-cc-pwCVQZ basis sets for [H,C,S,H] and [H,C,Se,H], respectively, while the energies correspond to the FPA final estimates. [c] A scale factor of 1.0979, taken from ref.[1], was employed for scaling ω_{TS}, i.e., the barrier curvature. In the case of HCOH, this simple scaling caused the computed Eckart-barrier half-life to coincide with experiment. [d] The experimentally determined[1] tunneling half-life is 2 h in between 11 and 20 K and in different matrices.

a noticeable tunneling in the case of *t*-HCSH. Since the Eckart-barrier parameters for *t*-HCSeH are rather similar to those of *t*-HCSH, the same test calculations for this system result in very similar findings. Overall, it can be concluded that in the *t*-HCXH → H_2CX series, the Eckart-barrier approach suggests very large tunneling half-lives for X = S and X = Se, making the observation of tunneling under matrix isolation conditions impossible.

A more appropriate and at the same time more elaborate and still only one-dimensional model of the tunneling motion employs the WKB approximation. The results obtained are presented in Table VIII. The different levels of electronic structure theory employed to determine the IRPs provide similar half-lives. The ZPVE corrections play a significant role in determining the WKB tunneling half-lives. It is important to point out that inclusion of motion perpendicular to the tunnelling path always makes the tunneling half-lives approximately an order of magnitude smaller. When the goal is to get quantitative agreement with experiment this is a large factor and thus it should be considered. Nevertheless, for preliminary, semi-quantitative tunneling half-lives the computation of these rather expensive corrections can be avoided.

The Eckart-barrier half-lives are always considerably larger than those determined by the WKB approximation. This is due to the fact that, at least for this series, the Eckart barriers, of set form, are wider than those determined by the IRP. The Eckart-barrier approach thus provides an upper bound to the tunneling half-lives and seems to be correct within about one-to-two orders of magnitude. This is deemed to be sufficient for most practical purposes as tunnelling half-lives vary over many orders of magnitude and systems which could show enhanced tunneling can clearly be identified this way.

The tunneling half-lives for the *t*-HCSD → HDCS and the *t*-HCSeD → HDCSe isomerization reactions are about 10 orders of magnitude larger than those involving the motion of H. This finding is very similar to that observed for *t*-HCOH and *t*-HCOD [1].

At higher temperatures the tunneling half-lives increase considerably but for the two systems investigated they remain large even at room temperature.

CONCLUSIONS

Despite numerous experimental attempts to synthesize *t*-HCSH via routes similar to those that resulted in the formation of the parent hydroxymethylene, this [H,H,C,S] isomer has thus far remained inaccessible under

matrix isolation conditions. The reaction of carbon atoms with H_2S similar to the approach utilized for the C + H_2O reaction[84] was equally unsuccessful and only the global minimum H_2CS could be observed. The structural results of the present study seem to indicate that part of the reason for not being able to synthesize *t*-HCSH is that it is not a true carbene and it is better represented as an ylide with a negatively charged carbon atom and a positively charged sulfur. This also reduces the driving force (exothermicity, ca. 44 kcal mol^{-1}) for the rearrangement to thioformaldehyde as compared to the rearrangement of *t*-HCOH to formaldehyde (ca. 52 kcal mol^{-1}). Similar arguments apply to *t*-HCSeH.

The most important results of the present computational study concern the unimolecular isomerization reactions of *t*-HCXH to H_2CX (X = S and Se). Comparison of the intrinsic reaction paths of the reactions *t*-HCXH to H_2CX (X = O, S, Se) indicate that the energetic characteristics of the paths are very similar. For example, the best estimates, obtained via the FPA approach, for the barriers to isomerization on the reactant side are 29.7, 33.2, and 29.7 kcal mol^{-1} for X = O, S, and Se, respectively. The barriers to isomerization on the product side are large, over 75 kcal mol^{-1}. The *cis*- and *trans*-HCXH forms are very similar in energy, the *trans* forms being more stable. The extra stabilities for X = {O, S, Se} are only {4.4, 1.0, 0.6} kcal mol^{-1}. The difference between the X = O and the X = S and Se numbers clearly reflect the different bonding characteristics of the species.

The computed results suggest unequivocally that tunneling is too slow for *t*-HCSH and *t*-HCSeH to be observable in matrix isolation experiments. In this sense, these congeners of hydroxymethylene are drastically different from the parent which is characterized by a fast tunneling process.

Similarly to what was observed for the *t*-HCOH → H_2CO unimolecular isomerization reaction[1], the very simple Eckart-barrier approach is successful in predicting tunneling half-lives to within one to two orders of magnitude. Since the characteristic half-lives vary over many orders of magnitude, this means that this simple approach, requiring simple characterization of only the stationary points of the tunneling reaction, can be successfully employed for the screening of candidate molecules for tunneling observable at the time-scales of normal matrix isolation studies. The one-dimensional WKB approximation provides reliable estimates for the temperature-dependent tunneling half-lives of the unimolecular isomerization reactions *t*-HCSH → H_2CS and the *t*-HCSeH → H_2CSe.

The work described was supported by an ERA Chemistry grant awarded to A.G.C. and P.R.S.. The work also received support from the Hungarian Scientific Research Fund (OTKA, K72885). The

European Union and the European Social Fund have also provided financial support to this project under Grant No. TÁMOP-4.2.1/B-09/1/KMR-2010-0003. We thank H. P. Reisenauer (Giessen) for attempting the preparation of HCSH through the reaction of H_2S with carbon atoms.

APPENDIX

Functional forms of the IRC curves for the unimolecular isomerization reactions *t*-HCXH → H_2CX, X = O, S, Se, given on Fig. 4 are as follows:

X = O: –62.8842 + 65.8252 Cos[x] – 18.2595 Cos[2x] + 21.0127 Cos[3x] – 8.52069 Cos[4x] + 2.89316 Cos[5x] + 0.423326 Cos[6x] – 0.939729 Cos[7x] + 0.649767 Cos[8x] – 0.234377 Cos[9x] + 0.0451329 Cos[10x] – 10.4899 Sin[x] – 7.06332 Sin[2x] + 17.0002 Sin[3x] – 15.2152 Sin[4x] + 11.0171 Sin[5x] – 6.15966 Sin[6x] + 2.69176 Sin[7x] – 0.870701 Sin[8x] + 0.17719 Sin[9x] – 0.0158624 Sin[10x];

X = S: –39.0463 + 30.2293 Cos[x] + 6.27172 Cos[2x] + 2.73431 Cos[3x] – 0.975252 Cos[4x] + 1.19851 Cos[5x] – 0.70709 Cos[6x] + 0.447667 Cos[7x] – 0.22289 Cos[8x] + 0.0915541 Cos[9x] – 0.0249896 Cos[10x] – 16.9685 Sin[x] + 9.66946 Sin[2x] – 2.76897 Sin[3x] + 2.009 Sin[4x] – 0.825287 Sin[5x] + 0.450519 Sin[6x] – 0.145358 Sin[7x] + 0.0496016 Sin[8x] – 0.00530263 Sin[9x] – 0.00192189 Sin[10x];

X = Se: –37.7913 + 30.3765 Cos[x] + 4.92309 Cos[2x] + 2.80322 Cos[3x] – 1.17426 Cos[4x] + 1.43368 Cos[5x] – 0.986103 Cos[6x] + 0.702098 Cos[7x] – 0.452469 Cos[8x] + 0.250845 Cos[9x] – 0.116907 Cos[10x] – 17.9695 Sin[x] + 10.1737 Sin[2x] – 3.2101 Sin[3x] + 2.44279 Sin[4x] – 1.10802 Sin[5x] + 0.713879 Sin[6x] – 0.288515 Sin[7x] + 0.127064 Sin[8x] – 0.0312082 Sin[9x] – 0.00449833 Sin[10x].

Note that these curves should only be considered in the following intervals: arc length ∈ [–1.74, 2.37], [–2.24, +2.68] and [–2.48, +2.83] for X = O, S and Se, respectively.

REFERENCES AND NOTES

1. Schreiner P. R., Reisenauer H. P., Pickard F. C., Simmonett A. C., Allen W. D., Mátyus E., Császár A. G.: *Nature* **2008**, *453*, 906.
2. Havlas Z., Kovář T., Zahradník R.: *J. Mol. Struct. (THEOCHEM)* **1986**, *136*, 239.
3. Judge R. H., Moule D. C., King G. W.: *J. Mol. Spectrosc.* **1980**, *81*, 37.
4. Hachey M. R. J., Grein F.: *Chem. Phys.* **1995**, *197*, 61.
5. Kaiser R. I., Ochsenfeld C., Head-Gordon M., Lee Y. T.: *Science* **1998**, *279*, 1181.
6. Ochsenfeld C., Kaiser R. I., Lee Y. T., Head-Gordon M.: *J. Chem. Phys.* **1999**, *110*, 9982.
7. Roothaan C. C. J.: *Rev. Mod. Phys.* **1951**, *23*, 69.
8. Møller C., Plesset M. S.: *Phys. Rev.* **1934**, *46*, 618.
9. Čížek J.: *J. Chem. Phys.* **1966**, *45*, 4256.

10. Crawford T. D., Schaefer H. F.: *Rev. Comput. Chem.* **2000**, *14*, 33.
11. Tachibana A., Okazaki I., Koizumi M., Hori K., Yamabe T.: *J. Am. Chem. Soc.* **1985**, *107*, 1190.
12. Cox A. P., Hubbard S. D., Kato H.: *J. Mol. Spectrosc.* **1982**, *93*, 196.
13. Johnson D. R., Powell F. X.: *Science* **1970**, *169*, 679.
14. Johnson D. R., Powell F. X., Kirchhoff W. H.: *J. Mol. Spectrosc.* **1971**, *39*, 136.
15. Maeda A., Medvedev I. R., Winnewisser M., DeLucia F. C., Herbst E., Müller H. S. P., Koerber M., Endres C. P., Schlemmer S.: *Astrophys. J. Suppl. Ser.* **2008**, *176*, 543.
16. Beers Y., Klein G. P., Kirchhoff W. H., Johnson D. R.: *J. Mol. Spectrosc.* **1972**, *44*, 553.
17. Johns J. W. C., Olson W. B.: *J. Mol. Spectrosc.* **1971**, *39*, 479.
18. Turner P. H., Halonen L., Mills I. M.: *J. Mol. Spectrosc.* **1981**, *88*, 402.
19. Torres M., Safarik I., Clement A., Strausz O. P.: *Can. J. Chem.* **1982**, *60*, 1187.
20. Flaud J. M., Lafferty W. J., Perrin A., Kim Y. S., Beckers H., Willner H.: *J. Quant. Spectrosc. Radiat. Transfer* **2008**, *109*, 995.
21. Harmony M. D., Laurie V. W., Kuczkowski R. L., Schwendeman R. H., Ramsay D. A., Lovas F. J., Lafferty W. J., Maki A. G.: *J. Phys. Chem. Ref. Data* **1979**, *8*, 619.
22. Fabricant B., Krieger D., Muenter J. S.: *J. Chem. Phys.* **1977**, *67*, 1576.
23. Martin J. M. L., Francois J. P., Gijbels R.: *J. Mol. Spectrosc.* **1994**, *168*, 363.
24. Carter S., Handy N. C.: *J. Mol. Spectrosc.* **1998**, *192*, 263.
25. Léonard C., Chambaud G., Rosmus P., Carter S., Handy N. C.: *Phys. Chem. Chem. Phys.* **2001**, *3*, 508.
26. Schreiner P. R., Reisenauer H. P., Romanski J., Mloston G.: *Angew. Chem. Int. Ed.* **2009**, *48*, 8133.
27. Rzepa H.: *J. Chem. Theory Comput.* **2010**, *7*, 97.
28. Brown R. D., Godfrey P. D., McNaughton D.: *Chem. Phys. Lett.* **1985**, *118*, 29.
29. Cox P., Hubbard S. D., Kato H.: *J. Mol. Spectrosc.* **1982**, *93*, 196.
30. Bock H., Aygen S., Rosmus P., Solouki B., Weissflog E.: *Chem. Ber.* **1984**, *117*, 187.
31. Glinski R. J., Taylor C. D., Martin H. R.: *J. Phys. Chem.* **1991**, *95*, 6159.
32. Beckers H., Kim Y. S., Willner H.: *Inorg. Chem.* **2008**, *47*, 1693.
33. Collins S., Back T. G., Rauk A.: *J. Am. Chem. Soc.* **1985**, *107*, 6589.
34. Yadav V. K., Yadav A., Poirier R. A.: *J. Mol. Struct.* **1989**, *186*, 101.
35. Brown R. D., Godfrey P. D., McNaughton D.: *J. Mol. Spectrosc.* **1986**, *120*, 292.
36. Kwiatkowski J. S., Leszczynski J.: *Mol. Phys.* **1994**, *81*, 119.
37. Leszczynski J., Kwiatkowski J. S., Leszczynska D.: *Chem. Phys. Lett.* **1992**, *194*, 157.
38. Judge R. H., Moule D. C.: *J. Am. Chem. Soc.* **1984**, *106*, 5407.
39. Yamada M., Osamura Y., Kaiser R. I.: *Astron. Astrophys.* **2002**, *395*, 1031.
40. Császár A. G., Allen W. D., Yamaguchi Y., Schaefer H. F. in: *Computational Molecular Spectroscopy* (P. Jensen and P. R. Bunker, Eds), pp. 15–68. Wiley, New York 2000.
41. Dunning T. H., Jr.: *J. Chem. Phys.* **1989**, *90*, 1007.
42. Kendall R. A., Dunning T. H., Jr., Harrison R.: *J. Chem. Phys.* **1992**, *96*, 6796.
43. Wilson A. K., van Mourik T., Dunning T. H., Jr.: *J. Mol. Struct.* **1996**, *388*, 339.
44. Woon D. E., Dunning T. H., Jr.: *J. Chem. Phys.* **1995**, *103*, 4572.
45. Kállay M., Surján P. R.: *J. Chem. Phys.* **2001**, *115*, 2945.
46. Purvis G. D., Bartlett R. J.: *J. Chem. Phys.* **1982**, *76*, 1910.
47. a) Noga J., Bartlett R. J.: *J. Chem. Phys.* **1987**, *86*, 7041; b) Erratum: Noga J., Bartlett R. J.: *J. Chem. Phys.* **1988**, *89*, 3401; c) Scuseria G. E., Schaefer H. F.: *Chem. Phys. Lett.* **1988**, *152*, 382.

48. Raghavachari K., Trucks G. W., Pople J. A., Head-Gordon M.: *Chem. Phys. Lett.* **1989**, *157*, 479.
49. Kállay M., Gauss J.: *J. Chem. Phys.* **2005**, *123*, 214105.
50. Bomble Y., Kállay M., Gauss J., Stanton J. F.: *J. Chem. Phys.* **2005**, *123*, 054101.
51. Császár A. G., Allen W. D., Schaefer H. F.: *J. Chem. Phys.* **1998**, *108*, 9751.
52. Allen W. D., East A. L. L., Császár A. G. in: *Structures and Conformations of Non-Rigid Molecules* (J. Laane, M. Dakkouri, B. van der Veken and H. Oberhammer, Eds), p. 343. Kluwer, Dordrecht 1993.
53. Császár A. G., Tarczay G., Leininger M. L., Polyansky O. L., Tennyson J., Allen W. D. in: *Spectroscopy from Space* (J. Demaison and K. Sarka, Eds), pp. 317–339. Kluwer, Dordrecht 2001.
54. Furtenbacher T., Czakó G., Sutcliffe B. T., Császár A. G., Szalay V.: *J. Mol. Struct.* **2006**, *780–781*, 283.
55. Ruscic B., Boggs J. E., Burcat A., Császár A. G., Demaison J., Janoschek R., Martin J. M. L., Morton M., Rossi M. J., Stanton J. F., Szalay P. G., Westmoreland P. R., Zabel F., Bérces T.: *J. Phys. Chem. Ref. Data* **2005**, *34*, 573.
56. a) Tarczay G., Miller T. A., Czakó G., Császár A. G.: *Phys. Chem. Chem. Phys.* **2005**, *7*, 2881; b) Erratum: Tarczay G., Miller T. A., Czakó G., Császár A. G.: *Phys. Chem. Chem. Phys.* **2008**, *10*, 7324.
57. Cowan R. D., Griffin D. C.: *J. Opt. Soc. Am.* **1976**, *66*, 1010.
58. Tarczay G., Császár A. G., Klopper W., Quiney H. M.: *Mol. Phys.* **2001**, *99*, 1769.
59. Scuseria G. E.: *J. Chem. Phys.* **1991**, *94*, 442.
60. Watts J. D., Gauss J., Bartlett R. J.: *J. Chem. Phys.* **1993**, *98*, 8718.
61. Gauss J., Stanton J. F.: *Chem. Phys. Lett.* **1997**, *276*, 70.
62. Stanton J. F., Gauss J., Harding M. E. and Szalay P. G., with contributions from Auer A. A., Bartlett R. J., Benedikt U., Berger C., Bernholdt D. E., Bomble Y. J., Cheng L., Christiansen O., Heckert M., Heun O., Huber C., Jagau T.-C., Jonsson D., Jusélius J., Klein K., Lauderdale W. J., Matthews D. A., Metzroth T., O'Neill D. P., Price D. R., Prochnow E., Ruud K., Schiffmann F., Schwalbach W., Stopkowicz S., Tajti A., Vázquez J., Wang F., Watts J. D.: *CFOUR, A Quantum Chemical Program Package*; the integral packages *MOLECULE* (Almlöf J., Taylor P. R.), *PROPS* (Taylor P. R.), *ABACUS* (Helgaker T., Jensen H. J. Aa., Jørgensen P. and Olsen J.), and ECP routines by Mitin A. V. and van Wüllen C. For the current version, see http://www.cfour.de
63. Kállay M.: *MRCC, A String-Based Quantum Chemical Program Suite*. See www.mrcc.hu for the latest version.
64. Liboff R. L.: *Introductory Quantum Mechanics*. Addison–Wesley, Reading (MA) 2003.
65. Razavy M.: *Quantum Theory of Tunneling*. World Scientific, Singapore 2003.
66. Fukui K.: *J. Phys. Chem.* **1970**, *74*, 4161.
67. Gonzalez C., Schlegel H. B.: *J. Phys. Chem.* **1990**, *94*, 5523.
68. Miller W. H., Handy N. C., Adams J. E.: *J. Chem. Phys.* **1980**, *72*, 99.
69. Allen W. D., Bődi A., Szalay V., Császár, A. G.: *J. Chem. Phys.* **2006**, *124*, 224310.
70. Eckart C.: *Phys. Rev.* **1930**, *35*, 1303.
71. *MATHEMATICA*, Version 4. Wolfram Research, Inc., Champaign (IL) 1999.
72. Kojima T., Nishikawa T.: *J. Phys. Soc. Jpn.* **1957**, *12*, 680.
73. Demaison J., Boggs J. E., Császár A. G. (Eds): *Equilibrium Molecular Structures*. CRC Press, Boca Raton 2011.
74. Gillespie R. J., Nyholm R. S.: *Q. Rev.* **1957**, *11*, 339.

75. Duncan J. L.: *Mol. Phys.* **1974**, *28*, 1177.
76. Seppelt K.: *Pure Appl. Chem.* **1987**, *59*, 1057.
77. a) Becke A. D.: *J. Chem. Phys.* **1993**, 98, 5648; b) Lee C., Yang W., Parr R. G.: *Phys. Rev. B* **1988**, 37, 785.
78. a) Krishnan R., Binkley J. S., Seeger R., Pople J. A.: *J. Chem. Phys.* **1980**, *72*, 650; b) Clark T., Chandrasekhar J., Spitznagel G. W., Schleyer P. v. R.: *J. Comput. Chem.* **1983**, *4,* 294.
79. Lide D. R. (Ed.): *CRC Handbook of Chemistry and Physics*, 88th ed. CRC Press Inc., Boca Raton, FL 2007.
80. McGurk J., Tigelaar H. L., Rock S. L., Norris C. L., Flygare W. H.: *J. Chem. Phys.* **1973**, *58*, 1420.
81. Czakó G., Nagy B., Tasi G., Somogyi A., Šimunek J., Noga J., Braams B. J., Bowman J. M., Császár A. G.: *Int. J. Quantum. Chem.* **2009**, *109*, 2393; and references therein.
82. Gerry M. C. L., Lees R. M., Winnewisser G.: *J. Mol. Spectrosc.* **1976**, *61*, 231.
83. Huber K. P., Herzberg G.: *Constants of Diatomic Molecules*. Van Nostrand Reinhold, New York 1979.
84. Schreiner P. R., Reisenauer H. P.: *ChemPhysChem* **2006**, *7*, 880.